

Generating Haar-Uniform Randomness Using Stochastic Quantum Walks on a Photonic Chip

Hao Tang^{1,2}, Leonardo Banchi^{3,4}, Tian-Yu Wang,^{1,2} Xiao-Wen Shang,^{1,2} Xi Tan,^{1,2} Wen-Hao Zhou,^{1,2} Zhen Feng,^{1,2} Anurag Pal,^{1,2} Hang Li^{1,2}, Cheng-Qiu Hu,^{1,2} M. S. Kim,^{5,6} and Xian-Min Jin^{1,2,7,*}

¹*Center for Integrated Quantum Information Technologies (IQIT), School of Physics and Astronomy and State Key Laboratory of Advanced Optical Communication Systems and Networks, Shanghai Jiao Tong University, Shanghai 200240, China*

²*CAS Center for Excellence and Synergetic Innovation Center in Quantum Information and Quantum Physics, University of Science and Technology of China, Hefei, Anhui 230026, China*


³*Department of Physics and Astronomy, University of Florence, via Giovanni Sansone 1, I-50019 Sesto Fiorentino (FI), Italy*

⁴*INFN Sezione di Firenze, via Giovanni Sansone 1, I-50019 Sesto Fiorentino (FI), Italy*

⁵*QOLS, Blackett Laboratory, Imperial College London, London SW7 2AZ, United Kingdom*

⁶*Korea Institute of Advanced Study, Seoul 02455, South Korea*

⁷*TuringQ Co., Ltd., Shanghai 200240, China*

 (Received 29 March 2021; revised 8 September 2021; accepted 3 January 2022; published 3 February 2022)

As random operations for quantum systems are intensively used in various quantum information tasks, a trustworthy measure of the randomness in quantum operations is highly demanded. The Haar measure of randomness is a useful tool with wide applications, such as boson sampling. Recently, a theoretical protocol was proposed to combine quantum control theory and driven stochastic quantum walks to generate Haar-uniform random operations. This opens up a promising route to converting classical randomness to quantum randomness. Here, we implement a two-dimensional stochastic quantum walk on the integrated photonic chip and demonstrate that the average of all distribution profiles converges to the even distribution when the evolution length increases, suggesting the 1-pad Haar-uniform randomness. We further show that our two-dimensional array outperforms the one-dimensional array of the same number of waveguide for the speed of convergence. Our Letter demonstrates a scalable and robust way to generate Haar-uniform randomness that can provide useful building blocks to boost future quantum information techniques.

DOI: [10.1103/PhysRevLett.128.050503](https://doi.org/10.1103/PhysRevLett.128.050503)

Random operations for quantum systems [1] play an important role for a large variety of tasks in quantum information processing. Especially, as various studies on boson sampling [2–7] have emerged in recent years to demonstrate quantum computational supremacy [8,9], the Haar random unitary matrices [10] required for these studies have drawn ever increasing attention. The Haar measure of randomness is now investigated as more than a theoretical tool, but also as a useful building block for quantum protocols or algorithms. It has wide applications covering boson sampling [2–4,6,7], quantum cryptography [11,12], quantum process tomography [13], entanglement generation [14], fidelity estimation [15], etc., which, therefore, motivated a series of experimental schemes on implementing random or pseudorandom quantum operations [16–18]. So far, these experimental schemes decompose a random unitary matrix either by using a large number of quantum gates [16–18] or using photonic beam splitters and interferometers [19,20] via Reck-Clements decomposition method [21,22], both of considerably high complexity in implementation.

An alternative approach to generate Haar-uniform random operations has recently been proposed [23], using

what we call a “stochastic quantum walk.” The rationale is based on quantum control theory, which allows for a coherent driving of permanently coupled quantum systems via classical control pulses and stochastic pulses. Instead of using quantum circuits or programmable photonic networks with beam splitters and phase shifters, in this alternative approach, random operations can be implemented via permanently coupled photonic waveguides by applying stochastic modulations. This scheme, which effectively implements a stochastic version of a continuous-time quantum walk [24], could be scalable and beneficial for practical quantum experiments including larger-scale boson sampling. However, up to now, this scheme has never been demonstrated in experiments.

Photonic lattice is an ideal physical platform to implement continuous-time quantum walk. A large evolution space in the photonic lattice allowing for real spatial two-dimensional (2D) quantum walks has been recently demonstrated [25,26]. While this physical system is suitable for coherent and pure quantum walks, the environmental decoherence term can also be intentionally introduced by lattice manipulation. The key process is to introduce classical randomness to the propagation constant along

different segments of each waveguide, which causes the randomness in the diagonal part of the Hamiltonian matrix. Therefore, a different kind of evolution, namely, the stochastic quantum walk, has been successfully demonstrated in the photonic lattice to simulate various open quantum systems [27,28].

In this Letter, we experimentally demonstrate an instance of Haar-uniform randomness using stochastic quantum walks on the integrated photonic chips. We prepare different samples with different random settings of the propagation constant and detunings, and then measure the light intensity distribution after the evolution inside each chip. The different samples created according to the above procedure yield different unitary evolutions that, in the ideal case, should represent independent samples from the Haar distribution. We show that the average of all distribution profiles converges to the even distribution when the evolution length increases, suggesting the one-pad Haar-uniform randomness. We further show that our 2D array outperforms the one-dimensional (1D) array of the same number of waveguide for the speed of convergence. Additionally, we analytically and numerically show convergence toward uniform distribution when injecting two or multiple indistinguishable photons into such photonic lattice. Our Letter demonstrates a highly scalable and robust physical implementation for generating Haar-uniform randomness, which can provide useful building blocks to boost future quantum information techniques.

The experimental scheme.—We start this section by briefly recalling the most stringent criterion to check when the averages over an ensemble of $N \times N$ unitary operators $\{U_i\}$ approximate the formal averages with respect to the Haar distribution. This is normally studied within the framework of approximate q designs [16,23,29] (see Supplemental Material Note 1 for more details [30]), which require a small distance between two particular averages,

$$\|\mathbb{E}_i[U_i^{\otimes q} \rho U_i^{\otimes q \dagger}] - \int_U U^{\otimes q} \rho U^{\otimes q \dagger} dU\|_{\diamond} < \varepsilon, \quad (1)$$

where $\|T\|_{\diamond}$ is the diamond norm of a superoperator T , ρ is the density matrix, and ε is the required small value. \mathbb{E}_i denotes the expectation value, i.e., the average over the ensemble of unitary operators. The second part refers to averages with respect to the Haar measure dU . We may also consider a weaker criterion by forcing ρ to be symmetric over permutations, to implement $U_i^{\otimes q} \rho U_i^{\otimes q \dagger}$ via experiments involving q indistinguishable photons, where the chip performs the same unitary to each indistinguishable particle.

Here we first focus on $q = 1$, which has important applications for quantum encryption [12], and we will briefly analyze $q > 1$ scenarios in later sections. The estimation of the diamond norm in Eq. (1) requires entangled photonic inputs and complete tomography,

which is challenging for experiments, as the measurement of each off-diagonal element requires different optical components [31]. For this reason, in Supplemental Material Note 1 [30], we introduce a weaker condition based on the $L2$ norm for which one can prove that entangled inputs are not required. Equation (S11) links the theoretical norm of $\mathbb{E}_i[U_i \rho U_i^{\dagger}] - I/N$ to our experimentally measured norm for M , namely, the distance between the diagonal elements and the uniform distribution (denoted as \mathcal{N}_d). There is another term in Eq. (S11) due to the off-diagonal part \mathcal{N}_{od} . The experiment for measuring the off-diagonal elements of $\mathbb{E}_i[U_i \rho U_i^{\dagger}]$ would be too complex, and we manage to show in Supplemental Material Note 2 and Fig. S1 [30] numerically that the off-diagonal elements for the photonic lattice model used in this Letter asymptotically converge to zero. Hence we focus on the experimental exploration on diagonal elements, which directly corresponds to the probability distribution at each waveguide and would experimentally verify whether these diagonal terms converge to zero.

For $q = 1$, the Haar average reduces to I/N , where N is the number of waveguides and I is the $N \times N$ identity matrix. Therefore, Eq. (1) demands

$$\|\mathbb{E}_i[U_i \rho U_i^{\dagger}] - I/N\|_d < \varepsilon \quad (2)$$

for all input states ρ , where $\|\cdot\|_d$ is the $L2$ norm of the diagonal elements. This is inspiring from the experimental perspective, as illustrated in Fig. 1(a). However, not all unitary ensembles can satisfy Eq. (2). For instance, quantum walks with a pure state input and an ensemble made by a single unitary have a fixed ballistic distribution rather than a uniform one. On the other hand, the theoretical proposal [23] shows that averages over different continuous-time stochastic quantum walks with sufficiently

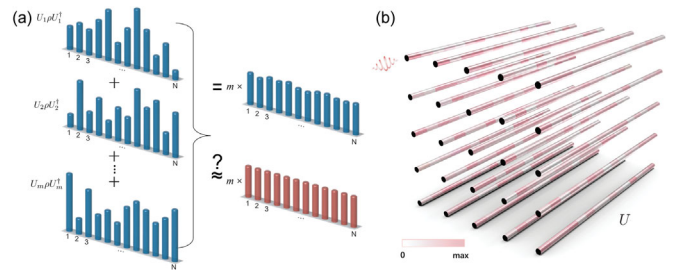


FIG. 1. Generating Haar-uniform randomness using stochastic quantum walks. (a) Illustration of averaging many stochastic quantum walks of a certain evolution time to reach the Haar measure. The red columns represent the distribution of I/N that appear in Eq. (2). (b) Schematic diagram of introducing random delta beta detunings to implement stochastic quantum walks on the photonic chip. The color bar shows the detuning strength of the propagation constant, where “max” corresponds to the given $\Delta\beta$ amplitude. Photons are injected into one waveguide, and the evolution in the lattice corresponds to a unitary operation.

long waveguides could successfully approximate the Haar averages.

Consider a photonic lattice where each waveguide is equally divided into the same number of segments, and each segment has a constant detuning of the propagation constant, with random detunings in all segments following a uniform distribution [see Fig. 1(b)]. The photon evolution through such a lattice with N waveguides corresponds to the operation with U of a size N . The evolution can be described by an effective piecewise Hamiltonian H_{eff} . For each segment k , there is

$$H_{\text{eff}}(k) = \sum_i^N [\beta_i - \Delta\beta_i(k)] a_i^\dagger a_i + \sum_{j \neq i}^N C_{ij} (a_i^\dagger a_j + a_j^\dagger a_i), \quad (3)$$

where β_i and C_{ij} are, respectively, the propagation constant and coupling coefficient for the lattice without any detunings. In practice, β_i is set the same for all waveguides. $\Delta\beta_i(k)$ is the constant detuning of the propagation constant for waveguide i at segment k , which can be experimentally achieved by tuning the writing speed (see details for $\Delta\beta$ tuning in Supplemental Material Note 3 and Fig. S2 [30]). The introduction of $\Delta\beta$ in H_{eff} has an effect of adding some classical dephasing terms during the evolution.

Thanks to Eq. (3), the unitary implemented by a chip of length $z = K\Delta z$ is $U(z) = (\prod_k e^{-iH_{\text{eff}}(k)\Delta z})$, where Δz is the length of each segment, and K is the number of segments. Calling $|\Psi(z)\rangle = U(z)|\Psi(0)\rangle$ for a given initial wave function $|\Psi(0)\rangle$, what is experimentally measured is the probability distribution $|\langle l|\Psi(z)\rangle|^2$ that the photon will come out from the l th waveguide after an evolution length z . The probability distribution is equivalent to the diagonal elements of $U\rho U^\dagger$.

In the experiment, we prepare photonic lattices of 5×5 waveguides, a total evolution length of 8 cm, and a segment length Δz of 2 mm. The random $\Delta\beta$ detunings in all segments follow a uniform distribution under a $\Delta\beta$ amplitude of 0.4 mm^{-1} using a femtosecond laser direct writing technique [5,25,32] (see details for waveguide preparation in Supplemental Material Note 4 [30]). In total, we have 17 random settings for the detuning profiles. We inject photons from one waveguide of the lattice and measure the evolution patterns for an evolution length of 1–8 cm, which will allow us to see how the performance changes with the evolution length. The experimental evolution patterns are given in Supplemental Material Figs. S3–S10 [30].

Result analysis.—As shown in Fig. 2, we measure the photonic evolution pattern for different evolution lengths after injecting a photon in the lattice of one random setting. We then read the intensity probability at each waveguide for each figure (see details in Supplemental Material

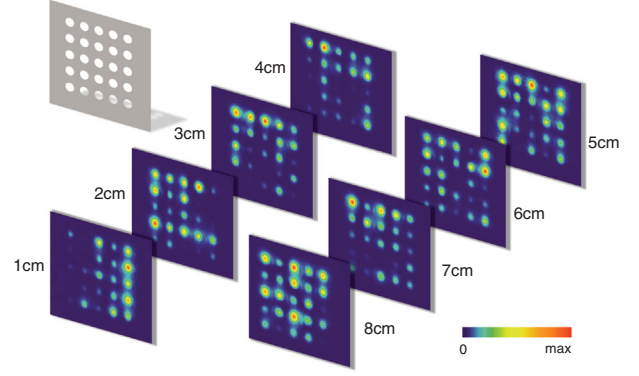


FIG. 2. Experimental results for stochastic quantum walks. The photonic evolution patterns of different evolution lengths for one random setting of photonic lattice. The corresponding evolution length of each graph is marked beside the graph. The mask illustrates how we read the figure data to get the probability distribution, with details explained in Supplemental Material Note 5 [30].

Note 5 [30]). We have processed all 17 random settings and each has 8 different evolution lengths.

For each evolution length, we average the probability distribution of the 17 settings. What we obtain is the diagonal part of $\mathbb{E}_i[U_i\rho U_i^\dagger]$ in Eq. (2). The diagonal part of the other term in Eq. (2) I/N can be viewed as the equal distribution at all 5×5 waveguides, which means each waveguide has an equal probability of 0.04. We subtract 0.04 from each element of the measured average probability distribution matrix, and we can get the diagonal part of $\mathbb{E}_i[U_i\rho U_i^\dagger] - I/N$, which is a 25×1 vector and can be written in a 5×5 matrix M .

We use the heat map to list the value of each element in the matrix M [see Fig. 3(a)]. Clearly, for a small evolution length, the fluctuation around zero for these element values is much more fierce than that for a larger evolution length. We calculate the $L2$ norm of M , i.e., $\|M\|$. If all elements in M are zero, $\|M\|$ will certainly be zero, while large deviations from zero in these elements make $\|M\|$ big. The calculated $\|M\|$ shown in Fig. 3(b) well supports the results in heat maps. $\|M\|$ gradually converges to a considerably small value when the evolution length increases. A slight gap between the experimental and numerical results may due to imperfect fitting for $\Delta\beta$ as explained in Supplemental Material Note 3 [30], but overall there is a good match to show that stochastic quantum walk results dynamically decay to zero. As a comparison, the pure quantum walk always keeps a high norm value and does not show a sign of convergence.

Our experiment demonstrates that the diagonal elements of $\mathbb{E}_i[U_i\rho U_i^\dagger]$ indeed tend toward a uniform distribution. We further show in Supplemental Material Note 7 and Figs. S11 and S12 [30] that, within a certain evolution length scale, increasing the evolution length lowers down the norm, before approaching a constant trend. Increasing

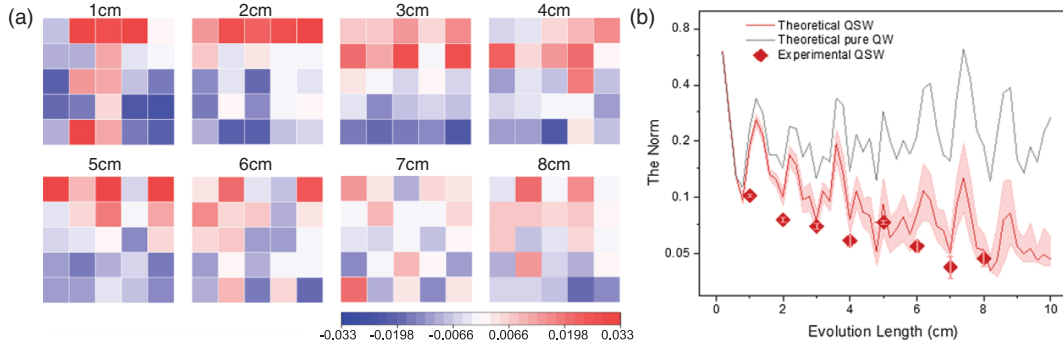


FIG. 3. Convergence to the Haar measure. (a) The heat maps show all the elements of the matrix M , the diagonal elements of $\mathbb{E}_i[U_i \rho U_i] - I/N$, for different evolution lengths z as shown above each heat map. The average for each z is estimated from 17 random settings with the same evolution length. Note that a few elements have a value above 0.033 or below -0.033 . They are represented in the heat map using the color for 0.033 or -0.033 , respectively. (b) The L2 norm $\|M\|$ for samples of different evolution lengths. QSW and QW stand for stochastic quantum walk and quantum walk, respectively. The theoretical results are obtained by setting Δz of 2 mm and averaging 17 random settings, which are consistent with the experiment. The shading area shows a possible range of theoretical results considering a 15% fluctuation of the $\Delta\beta$ amplitude; that is, the upper bound and lower bound of the shading area correspond to a $\Delta\beta$ amplitude of 0.34 and 0.46 mm^{-1} , respectively. The error bar for the experimental results is the standard error of the mean, with details explained in Supplemental Material Note 6 [30].

the $\Delta\beta$ amplitude can speed up the convergence without altering the norm lower bound, while increasing the number of samples can further lower down the norm. In Fig. S13, we show the segment length Δz also influences the convergence length without changing the norm lower bound. The convergence length does not monotonically change with Δz , but reaches a minimal value when choosing a proper Δz value. Our experiment demonstration of the diagonal elements, together with the numerical convergence of the off-diagonal part in Supplemental Material Note 2 [30], show that stochastic quantum walks can reach a one-design Haar measure at a long enough evolution length.

We further investigate the 1D photonic lattice of 1×25 waveguides [see Fig. 4(a)], a segment length Δz of 2 mm, and an evolution length of 8 cm. We set eight different $\Delta\beta$ amplitudes, namely, 0.1–0.8 mm^{-1} , and each has six random samples. The experimental patterns for all 1D samples are provided in Supplemental Material Fig. S14 [30]. We average the six probability distributions for each $\Delta\beta$ amplitude and plot their $\|M\|$ in Fig. 4(b). For the 1D array, as $\Delta\beta$ amplitude increases, there is a slightly reducing trend of the norm. We show in Fig. S15 a similar trend for the 2D lattices, that they converge better at a higher $\Delta\beta$ amplitude. This is because a stronger dephasing effect caused by larger $\Delta\beta$ detunings can facilitate a faster convergence to the Haar measure. However, the norm for 1D samples of large $\Delta\beta$ amplitudes still exceeds the norm for the 2D samples with a $\Delta\beta$ amplitude of 0.4 mm^{-1} . The 2D quantum walk has demonstrated the same ballistic transport with the 1D quantum walk, and yet a faster decay from the injection site than the latter. This is due to richer evolution paths [25] that also allow for more flexible Hamiltonian engineering [26]. In this Letter, we show that

the 2D stochastic quantum walk has a clear advantage in fast convergence to the Haar measure utilizing the rich evolution paths.

In addition, we explore the convergence to Haar measure for the scenario of $q > 1$ via some analytical and numerical analysis, as shown in Supplemental Material Note 8 and Fig. S15 [30]. The probability distribution when injecting

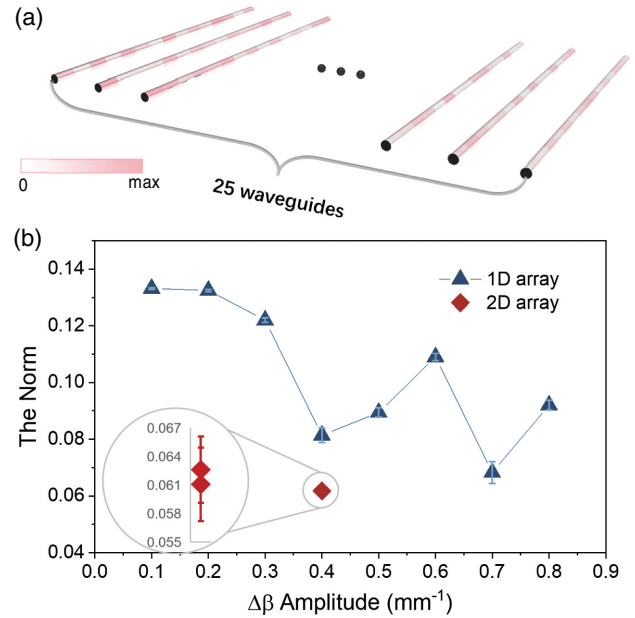


FIG. 4. Compare the performance in one- and 2D array. (a) Schematic diagram of the 1D photonic lattice of 25 waveguides with random tunings of the propagation constant. (b) The calculated L2 norm $\|M\|$ for 1D and 2D arrays. For 2D array, we get two sets of norm values, each by averaging six random settings separately.

two indistinguishable photons from mode i and i' would converge to $[2/N(N+1)]$. Alternatively, the compound light intensity at each mode j , I_j , would converge to $(2/N)$. The convergence follows the same dependence on the $\Delta\beta$ amplitude and on the number of groups as in $q=1$. Meanwhile, both $q=2$ and $q=1$ converge at a similar evolution length, showing the same convergence speed, as theoretically expected [23]. The difference lies in that the lower bound for $q=2$ is slightly higher. We further derive a general expression for the average probability; that is, $\prod_{k=1}^q [k/(N+q-k)]$, and (q/N) for the compound light intensity. They can be reduced to the aforementioned expression for $q=1$ or 2.

Discussion.—By taking full advantage of large-scale integrated photonic chips and precise lattice manipulation techniques, we manage to use the classical randomness (i.e., the random settings of $\Delta\beta$ detunings) to generate an important source for quantum randomness and make the unitary one-design distribution. That is, we have been able to demonstrate large-scale continuous-time stochastic quantum walks on the photonic chips and suggest the convergence to Haar-uniform randomness at a large evolution length.

Our approach offers a highly feasible alternative to the quantum gate approach or the Reck or Clements decomposition approach for generating Haar randomness. The Reck-Clements scheme offers a way of decomposing any certain unitaries to avoid the difficulties of constructing different configurations [33], and yet it requires fine-tuning of a quadratic number of parameters of beam splitters and phase shifters as the unitary scales up.

On the other hand, our approach does not need fine-tuning or complicated quantum circuit designs. Indeed, as long as the quantum walk Hamiltonian is “fully controllable,” namely, any unitary is reachable with proper local phases, random $\Delta\beta$'s with suitably long chips eventually yield Haar random unitary evolutions, without the need of precise phase calibration. Slightly different $\Delta\beta$ settings are mapped in fluctuations in the resulting unitary, which would also follow a Haar measure. Experimentally, we programmed the random $\Delta\beta$ with femtosecond laser writing speed. Even if the scale of detunings (the $\Delta\beta$ amplitude) is not kept as desired, after a long enough evolution (shown in Fig. S12), the average will still converge to the Haar measure. Meanwhile, the convergence can be improved with larger $\Delta\beta$ detunings, a properly selected segment length Δz , and more samples of different $\Delta\beta$ detunings. From Figs. S12 and S13, we see that a $\Delta\beta$ amplitude of 0.6 mm^{-1} with a Δz of 2 mm, or a $\Delta\beta$ amplitude of 0.4 mm^{-1} with a Δz of 5 mm, can both converge at a feasible evolution length below 10 cm. Therefore, we need to choose proper and feasible parameters considering today's fabrication technologies. Being free of fine-tuning and having feasible parameters are advantageous features for our approach.

In this Letter, we used many samples to compare ensemble averages with theoretical averages and proved convergence toward the Haar distribution. Nonetheless, a single Haar random chip is enough for most applications, e.g., boson sampling: once it is understood that noisy quantum walks converge toward the Haar distribution, in applications it is enough to fabricate a single chip, designed according to the theoretical recipe. Our experiment focuses on proving that noisy quantum walks do indeed converge toward the Haar distribution, and additionally, our analytical results show the convergence does apply to scenarios of multiple photons. Our utilization of 2D continuous-time stochastic quantum walk on photonic chips sheds light for more applications that need Haar randomness.

The authors thank Zi-Yu Shi for helpful discussion. This research is supported by National Key R&D Program of China (2019YFA0706302, 2019YFA0308700, 2017YFA0303700), National Natural Science Foundation of China (61734005, 11761141014, 11690033, 11904229), Science and Technology Commission of Shanghai Municipality (STCSM) (21ZR1432800, 20JC1416300, 2019SHZDZX01), and Shanghai Municipal Education Commission (SMEC) (2017-01-07-00-02-E00049). X.-M.J. acknowledges additional support from a Shanghai talent program and support from Zhiyuan Innovative Research Center of Shanghai Jiao Tong University. M. S. K.'s work is supported by the UK Hub in Quantum Computing and Simulation with funding from UKRI EPSRC Grant No. EP/T001062/1 and a Samsung GRC Grant. L. B. acknowledges support by the program “Rita Levi Montalcini” for young researchers.

*xianmin.jin@sjtu.edu.cn

- [1] T. Guhr, A. Müller-Groeling, and H. A. Weidenmüller, Random-matrix theories in quantum physics: Common concepts, *Phys. Rep.* **299**, 189 (1998).
- [2] J. B. Spring, B. J. Metcalf, P. C. Humphreys, W. S. Kolthammer, X. M. Jin, M. Barbieri, A. Datta, N. Thomas-Peter, N. K. Langford, D. Kundys, J. C. Gates, B. J. Smith, P. G. R. Smith, and I. A. Walmsley, Boson sampling on a photonic chip, *Science* **339**, 798 (2013).
- [3] M. A. Broome, A. Fedrizzi, S. Rahimi-Keshari, J. Dove, S. Aaronson, T. C. Ralph, and A. G. White, Photonic boson sampling in a tunable circuit, *Science* **339**, 794 (2013).
- [4] M. Tillmann, B. Dakić, R. Heilmann, S. Nolte, A. Szameit, and P. Walther, Experimental boson sampling, *Nat. Photonics* **7**, 540 (2013).
- [5] A. Crespi, R. Osellame, R. Ramponi, D. J. Brod, E. F. Galvão, N. Spagnolo, C. Vitelli, E. Maiorino, P. Mataloni, and F. Sciarrino, Integrated multimode interferometers with arbitrary designs for photonic boson sampling, *Nat. Photonics* **7**, 545 (2013).
- [6] N. Spagnolo, C. Vitelli, M. Bentivegna, D. J. Brod, A. Crespi, F. Flamini, S. Giacomini, G. Milani, R. Ramponi, P. Mataloni, R. Osellame, E. F. Galvão, and F. Sciarrino,

- Experimental validation of photonic boson sampling, *Nat. Photonics* **8**, 615 (2014).
- [7] H. Wang, Y. He, Y.-H. Li, Z.-E. Su, B. Li, H.-L. Huang, X. Ding, M.-C. Chen, C. Liu, J. Qin, J.-P. Li, Y.-M. He, C. Schneider, M. Kamp, C.-Z. Peng, S. Höfling, C.-Y. Lu, and J.-W. Pan, High-efficiency multiphoton boson sampling, *Nat. Photonics* **11**, 361 (2017).
- [8] A. W. Harrow and A. Montanaro, Quantum computational supremacy, *Nature (London)* **549**, 203 (2017).
- [9] J.-J. Wu, Y. Liu, B.-D. Zhang, X.-M. Jin, Y. Wang, H.-Q. Wang, and X.-J. Yang, A benchmark test of boson sampling on Tianhe-2 supercomputer, *Natl. Sci. Rev.* **5**, 715 (2018).
- [10] K. Życzkowski and M. Kuś, Random unitary matrices, *J. Phys. A* **27**, 4235 (1994).
- [11] P. Hayden, D. Leung, P. W. Shor, and A. Winter, Randomizing quantum states: Constructions and applications, *Commun. Math. Phys.* **250**, 371 (2004).
- [12] P. O. Boykin and V. Roychowdhury, Optimal encryption of quantum bits, *Phys. Rev. A* **67**, 042317 (2003).
- [13] A. Bendersky, F. Pastawski, and J. P. Paz, Selective and Efficient Estimation of Parameters for Quantum Process Tomography, *Phys. Rev. Lett.* **100**, 190403 (2008).
- [14] A. Hama, S. Santra, and P. Zanardi, Quantum Entanglement in Random Physical States, *Phys. Rev. Lett.* **109**, 040502 (2012).
- [15] C. Dankert, R. Cleve, J. Emerson, and E. Livine, Exact and approximate unitary 2-designs and their application to fidelity estimation, *Phys. Rev. A* **80**, 012304 (2009).
- [16] A. W. Harrow and R. A. Low, Random quantum circuits are approximate 2-designs, *Commun. Math. Phys.* **291**, 257 (2009).
- [17] J. Emerson, Y. S. Weinstein, M. Saraceno, S. Lloyd, and D. G. Cory, Pseudo-random unitary operators for quantum information processing, *Science* **302**, 2098 (2003).
- [18] R. N. Alexander, P. S. Turner, and S. D. Bartlett, Randomized benchmarking in measurement-based quantum computing, *Phys. Rev. A* **94**, 032303 (2016).
- [19] N. J. Russell, L. Chakhmakhchyan, J. L. O'Brien, and A. Laing, Direct dialling of Haar random unitary matrices, *New J. Phys.* **19**, 033007 (2017).
- [20] R. Burgwal, W. R. Clements, D. H. Smith, J. C. Gates, W. S. Kolthammer, J. J. Renema, and I. A. Walmsley, Using an imperfect photonic network to implement random unitaries, *Opt. Express* **25**, 28236 (2017).
- [21] M. Reck, A. Zeilinger, H. J. Bernstein, and P. Bertani, Experimental Realization of Any Discrete Unitary Operator, *Phys. Rev. Lett.* **73**, 58 (1994).
- [22] W. R. Clements, P. C. Humphreys, B. J. Metcalf, W. S. Kolthammer, and I. A. Walmsley, Optimal design for universal multiport interferometers, *Optica* **3**, 1460 (2016).
- [23] L. Banchi, D. Burgarth, and M. J. Kastoryano, Driven Quantum Dynamics: Will It Blend?, *Phys. Rev. X* **7**, 041015 (2017).
- [24] J. D. Whitfield, C. A. Rodríguez-Rosario, and A. Aspuru-Guzik, Quantum stochastic walks: A generalization of classical random walks and quantum walks, *Phys. Rev. A* **81**, 022323 (2010).
- [25] H. Tang, X.-F. Lin, Z. Feng, J.-Y. Chen, J. Gao, K. Sun, C.-Y. Wang, P.-C. Lai, X.-Y. Xu, Y. Wang, L.-F. Qiao, A.-L. Yang, and X.-M. Jin, Experimental two-dimensional quantum walk on a photonic chip, *Sci. Adv.* **4**, eaat3174 (2018).
- [26] H. Tang, C. Di Franco, Z.-Y. Shi, T.-S. He, Z. Feng, J. Gao, Z.-M. Li, Z.-Q. Jiao, T.-Y. Wang, M. S. Kim, and X.-M. Jin, Experimental quantum fast hitting on hexagonal graphs, *Nat. Photonics* **12**, 754 (2018).
- [27] F. Caruso, A. Crespi, A. G. Ciriolo, F. Sciarrino, and R. Osellame, Fast escape of a quantum walker from an integrated photonic maze, *Nat. Commun.* **7**, 11682 (2016).
- [28] H. Tang, Z. Feng, Y.-H. Wang, P.-C. Lai, C.-Y. Wang, Z.-Y. Ye, C.-K. Wang, Z.-Y. Shi, T.-Y. Wang, Y. Chen, J. Gao, and X.-M. Jin, Experimental Quantum Stochastic Walks Simulating Associative Memory of Hopfield Neural Networks, *Phys. Rev. Applied* **11**, 024020 (2019).
- [29] F. G. S. L. Brandão, A. W. Harrow, and M. Horodecki, Local random quantum circuits are approximate polynomial-designs, *Commun. Math. Phys.* **346**, 397 (2016).
- [30] See Supplemental Material at <http://link.aps.org/supplemental/10.1103/PhysRevLett.128.050503> for more details on the experiment, more figures on the experimental results, and for the analysis of the theoretical convergence.
- [31] I. Pitsios, L. Banchi, A. S. Rab, M. Bentivegna, D. Caprara, A. Crespi, N. Spagnolo, S. Bose, P. Mataloni, R. Osellame, and F. Sciarrino, Photonic simulation of entanglement growth and engineering after a spin chain quench, *Nat. Commun.* **8**, 1569 (2017).
- [32] Z. Chaboyer, T. Meany, L. G. Helt, M. J. Withford, and M. J. Steel, Tunable quantum interference in a 3D integrated circuit, *Sci. Rep.* **5**, 9601 (2015).
- [33] N. C. Harris, G. R. Steinbrecher, M. Prabhu, Y. Lahini, J. Mower, D. Bunandar, C. Chen, F. N. C. Wong, T. Baehr-Jones, M. Hochberg, S. Lloyd, and D. Englund, Quantum transport simulations in a programmable nanophotonic processor, *Nat. Photonics* **11**, 447 (2017).